Research Article

The dynamical evolution of Sudden Stratospheric Warmings of the Arctic winters in the past decade 2011–2021

R. Roy[1,2] · J. Kuttippurath[1]

Received: 8 November 2021 / Accepted: 16 February 2022
Published online: 14 March 2022

Abstract

In this study, we analyse the dynamical evolution, and identify the major warming (MW) and minor warming events of the past 11 Arctic winters (2010/11–2020/21). During the period, MW is found in 4 winters and is in January for 2012/13, 2018/19 and 2020/21 and in February for 2017/18. A major final warming is observed in the year 2015/16. The most severe MW occurred in the 2012/13 winter, for which a rise in temperature of about 30 K is found at 60° N. The investigation of tropospheric wave forcings for the period reveals that the MW in 2012/13 and 2017/18 is forced by the combined activity of waves 1 and 2, whereas the MW in 2018/19 and 2020/21 is driven by wave 1. Studies have shown that the frequency of Sudden Stratospheric Warming (SSW) in the Arctic has been increasing since 1957/58, which is about 1.1 MWs/winter during 1998/99–2009/10. However, this frequency decreases to 0.36 MWs/winter in the period 2010/11–2020/21 and 0.74 MWs/winter in 1998/99–2020/21. An inverse relationship is observed between the period of occurrence of SSWs and total column ozone (TCO) in the Arctic for the past 11 winters (2010/11–2020/21). For instance, the temperature in the lower stratosphere in January, in which most warmings occur, shows a statistically significant high positive correlation (0.79) with the average TCO in January–March. Therefore, this study assists in understanding the relationship between inter-annual variability of ozone and the occurrence of SSWs.

Article Highlights

- Major warmings (MWs) of the past decade occurred mostly in January and then in February.
- A decreasing trend in the occurrence of MWs in the past decade, 0.36 MWs/winter.
- The warming occurrences in the stratosphere make lower ozone depletion.
- A positive correlation exists between lower stratospheric temperature and total ozone.

Keywords Stratospheric Warming · Climate change · Polar vortex · Arctic · Ozone hole · Dynamics

Supplementary Information The online version contains supplementary material available at https://doi.org/10.1007/s42452-022-04983-4.

✉ J. Kuttippurath, jayan@coral.iitkgp.ac.in | [1]CORAL, Indian Institute of Technology Kharagpur, Kharagpur 721302, India. [2]Department of Physical Oceanography, Cochin University of Science and Technology, Kochi, India.

1 Introduction

The presence of Sudden Stratospheric Warming (SSW) events drives the dynamic nature of Arctic stratosphere in most winters. Scherhag [1] recorded the first of such warming, which takes place when the temperature rises suddenly at 10 hPa pressure level poleward of 60° N/S latitude in a matter of a few weeks [2]. The meridional temperature gradient is reversed, and the direction and speed of the zonal winds are changed during the major SSW period [3, 4]. The observed temperature increase is in the range of 30–40 K at 60°–90° N/S latitude, and it is followed by a reversal of westerlies during major warming (MW), but only a weakening of the westerlies during minor warming (mW) [5, 6]. Despite the WMO criterion for SSW, there are still debates on certain conditions chosen such as the latitude and duration of wind reversal [7–9]. The polar vortex dynamics and positions are altered by SSW-related changes in the westerlies, which finally culminate in either the displacement or breaking of the vortex [10–12].

The wave mean flow interactions between the climatological westerlies and the planetary waves is the actuating mechanism of SSWs. The westerlies of the polar vortex are forced by quasi-stationary waves (Rossby waves), resulting in a slowing of the winds and thus, the adiabatic warming there [13]. The vortex regains its shape and location depending on the type of wave forcings (e.g. wave number 1, 2 or 3). The classification of MW events to the split and displacement types differ based on the criterion such as the central dates and datasets used. For instance, the MW in 2009/10 (central date 9 February 2010) is identified as a displacement event in the study of Kuttippurath and Nikulin [7], but a vortex split event in other studies [14, 15]. They followed the criteria that closely resembled Charlton and Polvani [12] (CP07). The CP07 criterion classifies the events depending on the absolute vorticity of polar vortex. Unlike this, in the years following, the events were also classified based on the type of wave forcing causing the event. The vortex split events are often found associated with wave 2 forcing and displacement events are related to wave 1 forcing [16]. However, in a few winters, the split events were not forced by wave 2, but by wave 1 (e.g. 2018/19). Recently, another method of classifying the events was also devised by Choi et al. [17], where the MW occurrences are categorised as split and displacement events based on the nature of vortex and wave forcing (1 or 2) before and after the central dates.

SSWs are more common in the Northern Hemisphere (NH) than in the Southern Hemisphere (SH) due to strong planetary wave forcing in NH [18]. The two main elements that encourage this disparity are the difference in land and sea temperatures, as well as the topographical variations in these regions. The El Nino Southern Oscillation (ENSO), Quasi-Biennial Oscillation (QBO), sea ice concentration (SIC) and sea surface temperature (SST) anomalies also influence the wave forcing [19–24]. Climate change has a different effect on SSW events in NH than it does in SH. In a changing climate context, the SSW events tend to become more common in NH although no clear evidence has surfaced yet [25, 26]. An inherent consequence of SSW is noticeable in the surface climate for a few weeks or months [23, 27]. Aside from the effects on the surface temperature and precipitation, similar effects can be observed in the upper atmosphere such as in the mesosphere and ionosphere [28].

The occurrence of SSW has been increasing since its earliest documentation in January 1952. This rate of increase in frequency differs in different studies based on the criterion chosen for the classification of warming. The most used metric to classify the SSW into MW and mW is CP07, where the warming is considered to be major when the wind reverses at 10 hPa at the 60° N/S latitude from November to April, and must reverse for at least 10 days continuously before late April. However, the number of MWs can differ based on datasets. The assessment of reanalysis datasets for the period 1958–2002 conducted by CP07 shows that the SSW occurs in the order of six events per decade. Studies have also shown that SSW occurred once every two winters from the late 1950s to 1990 [14, 29]. Conversely, a single minor warming episode (1989/1990) was observed during the period 1989/90–1997/98 [30]. The warmings became more common beyond this period i.e., 1998/99–2008/09 [7]. Several winters were marked by the presence of multiple SSWs such as in 1998/99, 2001/02, 2007/08 and 2009/10 [31–34]. The study of Kuttippurath and Nikulin [7] revealed that the frequency of SSW in 1998/99–2009/10 (~ 1.1 MWs/winter) increased by nearly twice that recorded in 1957/58–1997/98 (~ 0.6 MWs/winter). Statistical characteristics of SSWs using model simulations and reanalysis showed that there is a high frequency of SSWs before the 1990s with an average of 5–6 events in a decade [35]. Similar model results of the SSW frequency are also presented in the study of Liu et al. [36]. All three studies show that the majority of these warmings occur in the month of January, followed by February.

Here, we analyse the SSWs occurred during the period 2010/11–2020/21. We perform a comprehensive analysis of all minor and major warmings that have happened in the past decade. Four major warmings were recorded in the winters of 2012/13, 2017/18, 2018/19 and 2020/21 [37–42]. The impact of SSW on the Arctic ozone and the frequency of SSWs over the course of time are evaluated. The first section of the study examines the temporal

evolution of meteorological parameters. The polar vortex dynamics is an inevitable component in the analysis of SSWs, and thus the Potential Vorticity (PV) maps are examined afterwards. The dynamical evolution of the fluxes is described in the last part of the first section and is crucial to understanding the wave components of dynamical forcing. The last part concludes with an examination of the relationship between ozone concentration and SSW timings (Table 1).

2 Data and methods

The Charlton and Polvani (CPO7) [12] criterion is applied to classify the winters as major warming and minor warming. When the temperature rises rapidly (20–30 K) North and South of 60° N/S and is accompanied by a reversal of zonal winds at 10 hPa, the event is a MW. Warming is referred to as a mW when the reversal of zonal winds does not accompany the increase in temperature. We use the Modern-Era Retrospective Analysis for Research and Applications (MERRA-2) data to investigate the changes in temperature and zonal winds [43]. These reanalysis datasets have a resolution of 0.5°×0.625° and a temporal resolution of three hours at 42 pressure levels. The classification of events based on the nature of polar vortex position and movements is similar to that of Cohen and Jones [14]. The breaking of a polar vortex during spring, and thus, the change in the direction of the zonal winds, characterise the final warming [44]. The final warming dates are analysed in our study based on the date of final reversal of the westerly at 10 hPa in the 65° N latitude, as done by Black and Daniel [45]. As a result, once the westerlies shift to easterlies due to the final warming, they will prevail until the next autumn.

Apart from this, the dynamical evolution of the winters is analysed using the Eliassen Palm (EP) flux divergence, heat flux, momentum flux and the amplitudes of wave forcings. The EP flux analysis assists in the estimation of tropospheric wave forcing. Detailed descriptions of this are found in Andrews et al. [4]. The divergence of EP flux is calculated using the method devised by Jucker [46]. Different methods of scaling the flux vectors are also described in other studies [47]. The EP flux considered in our study combines the vertical and meridional components. The dynamics of the vortex is examined to identify the years of vortex split and displacement using the PV maps [48]. The vortex edge is estimated by the Nash et al. [49] criteria. These maps are overlaid using the geopotential heights taken from the MERRA 2 data.

The relationship between the concentration of ozone and the presence of MW in the winters is evaluated using the total column ozone (TCO) obtained from the TOMS (Total Ozone Mapping Spectrometer), OMI (Ozone Monitoring Instrument) and OMPS (Ozone Mapping and Profiler Suite) satellite instruments. The trend in TCO is evaluated for the past four decades and correlation of the TCO with temperature, wind, Area of the Polar Stratospheric Clouds (A_{psc}) and the geopotential height (GPH) is estimated using the linear regression method. The mean PSC area (A_{psc}) at 460 K computed from the MERRA-2 dataset is taken from the NASA ozone watch website. The statistical significance of the relationship between the parameters and TCO is evaluated using the two-tailed t-test.

3 Dynamics of the winters

3.1 Temperature and zonal winds

3.1.1 Warmings during the winters 2010/11–2020/21

The evolution of zonally averaged temperature for the winters of 2010/11–2020/21 at 60° N and 90° N is presented in Fig. 1. Individual years are shown in different colours and the third panel of Fig. 1 shows the seasonal development of mean zonal winds at 60° N. The significance of examination at 90° N is to analyse the amplification effect of the change in temperature due to SSW in the polar region. Climatology of the temperature and zonal winds is also presented in Fig. 1, to better understand the inter-annual variability. The estimates of zonal wind speed at 60° N reveal that the winters 2012/13, 2017/18, 2018/19 and 2020/21 were characterised by the reversal of wind. The most severe and prolonged warming was in 2012/13. The temperature at 60° N began to increase by late December (202 K) (20–24 December) and it reached the peak of warming in early January (234 K, 10–11 January). Therefore, a rise of about 30 K was observed in that winter [38]. However, the next MW was observed after 4 years, in 2017/18 and temperature rise of about 24–26 K (60° N) was found in the winter (214–238 K, early February to mid-February). Model predictions of Rao et al. [44] and Karpechko et al. [50] also estimated similar dates of onset for the MW in that winter. The warming in 2018/19 and 2020/21 began in mid-December and continued until early January. Unlike the previous warmings, the rise in temperature at 60° N for both winters was moderate in the range of 20 K (210–230 K). Contrary to this, the temperature rise almost doubled at 90° N for both 2020/21 (38 K) and 2018/19 (40 K) MWs, and the intensity of warming at 90° N was lower for 2012/13 and 2017/18.

Apart from the major warmings, minor warmings were also observed during the period of study. A temperature difference of 20 K was noticed at 90° N in 2010/11 and 2019/20 from late January to early February. However, the

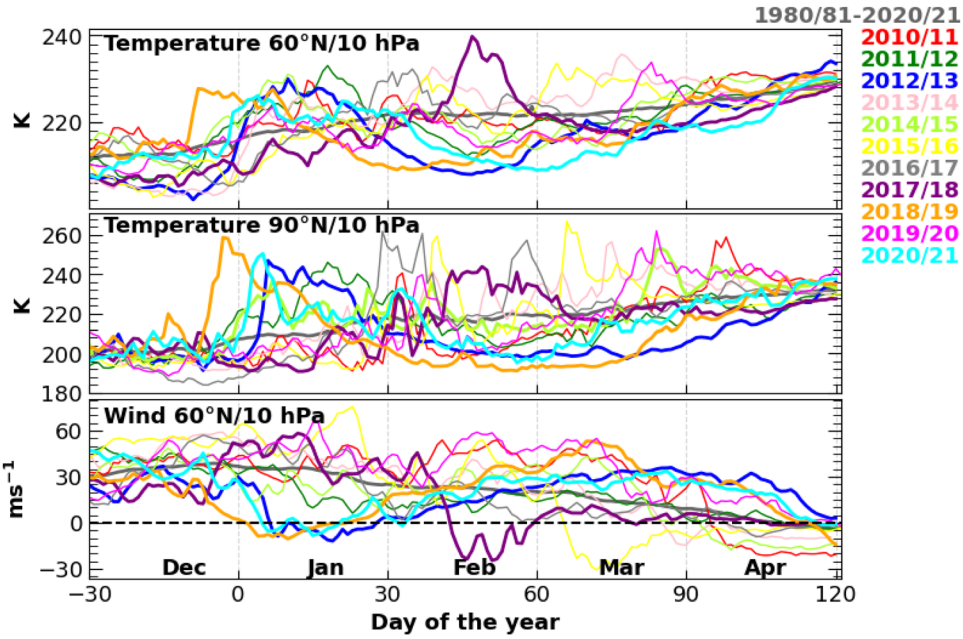

Fig. 1 Temporal evolution of temperature at 60° N and 90° N latitude at 10 hPa and the evolution of zonal winds at 60° N at 10 hPa (data: MERRA 2). The dashed horizontal line in the bottom panel represents zero velocity and the vertical dashed line is indicative of each month. The bold gray line in the background indicates the climatology (1980/81–2020/21)

temperature dropped soon after the warming, and thus, the winters experienced unprecedented ozone loss [51, 52]. The 2019/20 year was characterised by a cold late winter–spring, and experienced large loss in ozone during the period. The 2011/12 winter had a similar mW from early to mid-January and showed an increase of 22 K at 90° N. The presence of mW during these winters is more prominent at 90° N. Temperature increase in 2014/15 and 2016/17 was featured by a rise similar to that observed in MWs (see Manney et al. [53]). The temperature increased from 206 to 230 K and from 210 to 230 K at 60° N during early January to early February in 2017, and late December 2013 to early January 2014, respectively. Similar observations of the rise in temperature during MWs and mWs are also illustrated in Fig. S1 of the supplementary data.

A unique major final warming (MFW) event was observed in 2015/16 when the temperature rose close to 20 K at 60° N and 40 K at 90° N. A major final warming event occurs when the polar vortex disrupts early in spring and does not recover later in the season [54]. The reversal of westerlies following the intensification of warming occurs after the lag of a few days. For instance, the earliest MW among the 11 years of study is observed in 2012/13. The easterlies appeared on 6 January 2013 (5–10 ms^{-1}) a few days after the onset of warming and continued for few weeks. Easterlies first appeared on 12 February 2018, 2 January 2019 and 5 January 2020 in the other MW winters. The easterlies stayed longest in 2012/13 (22 days) followed by 2018/19 winter (21 days). The westward winds in 2017/18 persisted for about 19 days and 13 days (2 days of westerlies were present in between) in 2020/21 [55, 56]. The MFW observed in 2015/16 was one of the earliest final warmings observed in the Arctic for the past two decades. The zonal winds decelerated; coinciding with the periods of mW in other winters as depicted in Fig. 1. The westerlies were strong (30–60 ms^{-1}) in early winter in 2010/11, 2015/16 and 2019/20; implying a stronger polar vortex in these winters. The final warming for the winters 2010/11, 2013/14, 2014/15, 2016/17 and 2017/18 occurred in late March and early April, but late April for the years 2011/12, 2012/13, 2019/20 and 2020/21.

3.1.2 Vertical development of the major warmings

Figure 2 shows the vertical development of the zonally averaged temperature (coloured contours [left]) from 60° N to 90° N along with the evolution of the westerlies and easterlies (coloured contours [right]) (zonally averaged over 60°–90° N). As discussed in much of the previous studies, following a MW event, the high-temperature regions descent to lower altitudes and is also accompanied by the descent of the easterlies. The extent of descent to the lowermost altitudes depends on the severity of warming and they remain in the same altitude for a short period (a week or more). During the 2012/13 winter, the easterlies appeared in late January and extended to altitudes as low as 75 hPa, as depicted in Fig. 2. The higher temperature contours of 240–250 K are found near the upper stratosphere (1–10 hPa). The lowermost descent of easterlies is observed during the MW of 2017/18. The high-temperature contours were found at altitudes lower than 10 hPa and the easterlies were present at altitudes lower than 75 hPa. Similar descent is also found in 2020/21, but is not as strong as the MW in 2017/18. The descent of easterlies

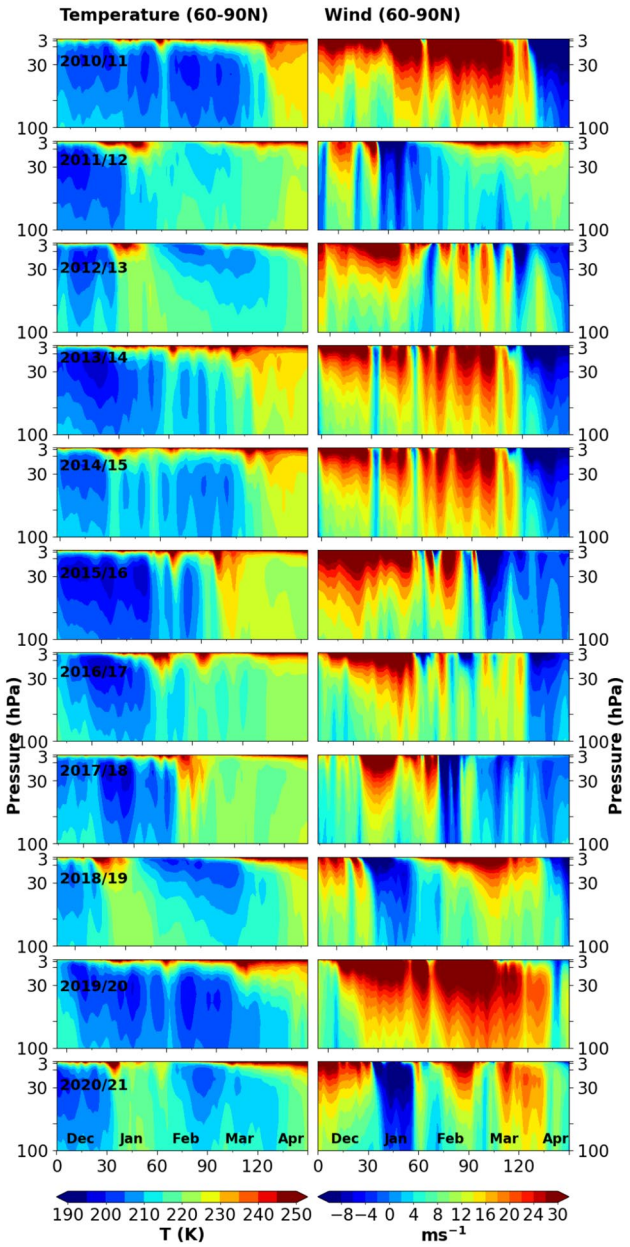

Fig. 2 Temporal evolution of the zonally averaged temperature and zonally averaged wind (60°–90° N) (data: MERRA 2) for the Arctic winters 2010/11–2020/21

in 2018/19 is limited to 75 hPa. Corresponding to the timings of mW the easterlies appeared in the upper stratosphere in 2013/14 and 2014/15, but are not classified as MW because the reversal of winds was short-lived. The MW in 2015/16 is highlighted by the presence of easterlies that descended to lower than 30 hPa and stayed intact until spring. However, the strength of easterlies (1–10 ms^{-1}) was lower than the westerlies (10–40 ms^{-1}) observed before the warming. Lower temperatures (196–206 K) were present throughout early winter in the years 2010/11, 2015/16 and 2019/20. Accelerated descent of high temperatures (225–240 K) is also noticed for the mW winters 2011/12, 2013/14 and 2016/17.

3.2 Potential vorticity analysis

A majority of SSW episodes conclude with either a split or displacement of the polar vortex. These changes in the vortex are significant because they assist to determine the severity of warmings, which can affect regional weather, and can aid in the diagnosis of wave forcings. These can be studied effectively using the PV maps. We have computed the Ertel's potential vorticity (EPV, 1 EPV = 10^{-3} PVU) (1 PVU is 10^{-6} km^2 kg^{-1} s^{-1}) from the MERRA 2 data for the MW winters (2012/13, 2017/18, 2018/19 and 2020/21) on selected dates at two different altitudes, as demonstrated in Figs. 3 and 4 for 10 hPa and 70 hPa, respectively. The temporal development of polar vortices is visible more discreetly at 10 hPa, and is discussed for three specific dates. For each year, the initial formation and dissipation of the vortex is examined on 15 December and 15 March, respectively. The central date is also marked, which indicates the date on which the zonal wind changes its direction. That is, the date corresponding to the westerlies at 10 hPa in 60° N latitude change their direction to easterlies. The geopotential height contours are superimposed on the PV maps. Geopotential height values are higher over warmer regions and vice versa. These contours closely follow the shape of polar vortex. Figure 3 shows the temporal evolution of polar vortex at 10 hPa. The early stages of the formation of vortex are observed for all MW winters. The vortex is observed to be circular and concentric in the beginning of warming in 2012/13 and 2017/18. However, the vortex is distorted to a coma-shaped and elongated for the 2018/19 and 2020/21 winters, respectively. In the lower altitudes or at 70 hPa the distinct concentric shapes of vortices are hardly identifiable (Fig. 4).

The vortex was stable in early December 2012 and was fully formed by the end of December as observed from Fig. 3**.** The MW in 2012/13 begun in late December and reached the peak stage during early January. Thus, as the westerlies changed to easterlies, the vortex became unstable and started to elongate (6 January 2013). Furthermore, on 8 January 2013, the vortex split and migrated to the mid-latitudes. A part of the vortex moved to Central North America and the other lobe displaced to Russia [37]. This split in the vortex and displacement to the nearby regions are also visible at 10 hPa. In 2017/18, a fully developed vortex is observed in December and as the warming begins, the vortex became less stable and split into two lobes on 12 February 2018 [41, 57]. The split is very evident at 10 hPa (Fig. 3), but less identifiable at 70 hPa (Fig. 4). The

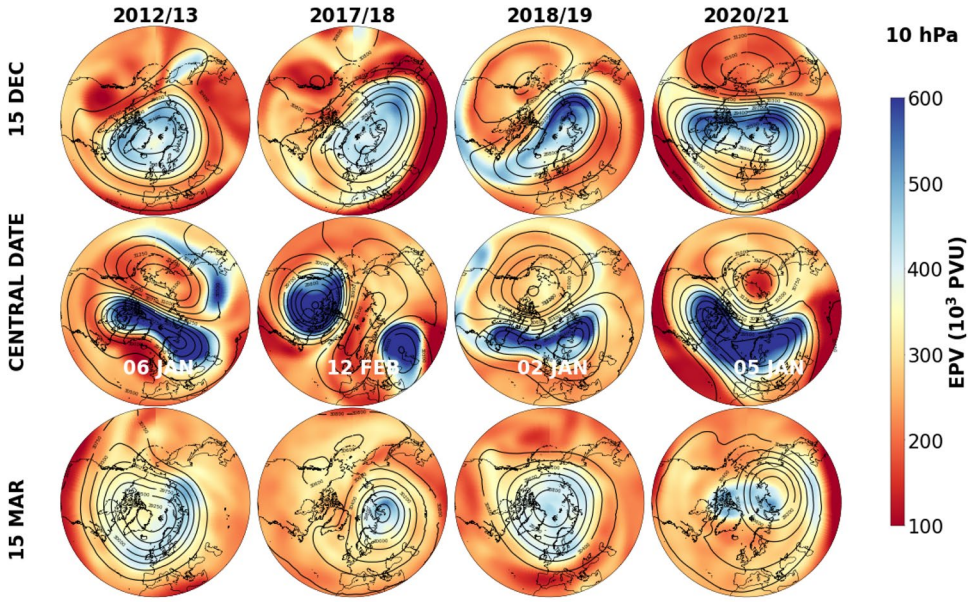

Fig. 3 Maps of potential vorticity (data: MERRA 2) at 850 K (~ 10 hPa/30 km/850 K) for various Arctic winters on 15 December, 15 March, and on the central date, the day on which the westerlies changed to easterlies at 60° N/10 hPa. The overlaid black contours show the geopotential height

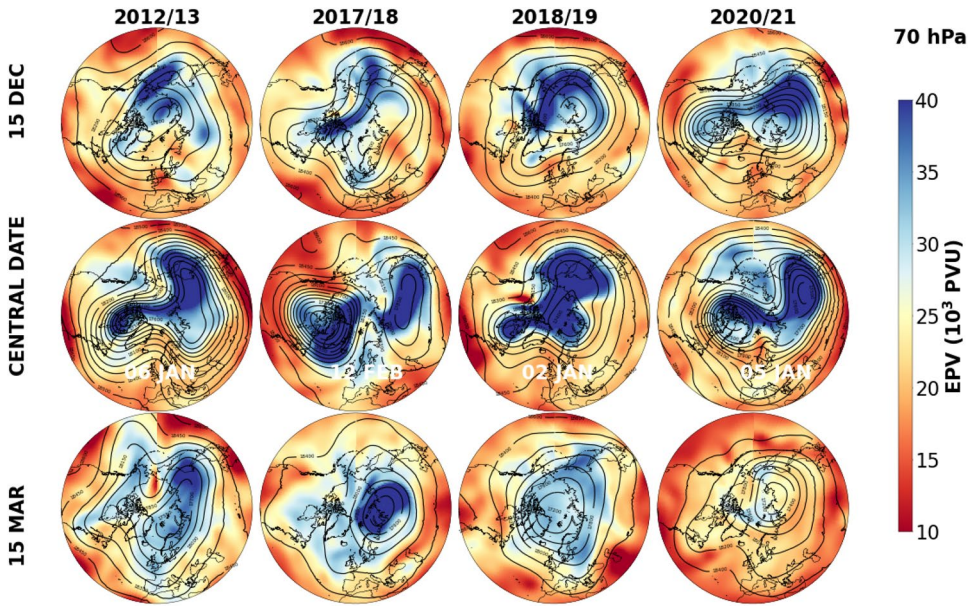

Fig. 4 Evolution of the PV maps for the similar period as depicted in this figure, but for the 70 hPa/17 km/475 K altitude

split became more explicit at both latitudes in the days following as the easterlies extended to lower altitudes, as illustrated in Fig. 2. The breaking of vortex in early (4) January of 2019 owing to MW that commenced in mid-December led to the shift of vortex to the eastern North America and Russia. The evolution of geopotential height with warming is also presented in the study of Lee and Butler [55]. Unlike the three years of MW (2012/13, 2017/18 and 2018/19), the MW in 2020/21 culminated into a displacement event. The warming soared up by late December and reached its peak intensity in early January and therefore, the vortex is displaced to the Eurasian continent. This change in position is apparent at both altitudes (Figs. 3, 4).

The dissipation of the vortex is observed around 15 March in all years. The vortex started to disappear slowly at 70 hPa compared to that at 10 hPa. The vortex almost disintegrated on 15 March 2018, but it is slower for the other warm winters. The vortex dissipated slowly in 2012/13 and 2019/20 due to the decrease in temperature soon after the warming and strengthened zonal winds.

3.3 Eliassen Palm flux divergence and wave forcings

A significant component influencing the variability of polar vortex and its position is the intensity of wave forcings from the lower latitudes [20, 58]. Therefore, the estimation of flux divergence and wave forcings are inevitable elements in the assessments of SSWs. The heat flux, momentum flux, amplitudes of the geopotential waves and the EP flux divergences are examined by considering their temporal progression at 60° N and 10 hPa, and are depicted in Fig. 5. The EP flux divergence is important also from the perspective of zonal winds. That is, negative values of EP flux divergence imply that the westerlies are decelerated (convergence) or that the westerlies could revert to easterlies. Conversely, positive values of EP flux divergence suggest strong westward winds or acceleration of the westerlies. Therefore, the EP flux divergence is significant to study the dynamics of polar vortex. The first panel of Fig. 5 shows the heat flux for the years 2010/11–2020/21. The heat flux increases up to the order 500–550 Kms^{-1} during the period of warming in 2012/13 and are the highest among the winters [59]. The corresponding momentum flux also increases to reach the peak value of 400 ms^{-1} in late December and early January. The heat flux (400–500 Kms^{-1}) and momentum flux (300–400 ms^{-1}) magnitudes in 2017/18 and 2018/19 are very similar, but are slightly lower in 2020/21 (300–400 Kms^{-1} and 200–300 ms^{-1}, respectively). An interesting feature noticed is the high heat flux at 10 hPa and the highest momentum flux just before the peak warming period in all years, as also noted by Kuttippurath and Nikulin [7]. The estimates of mean zonal (45°–75° N) eddy heat flux at 100 hPa by Lu et al. [42] reveal an intensification of these fluxes right before the MW in 2020/21. A similar analysis is also present in the study of Lee and Butler [55] for the 2018/19 winter, where enhanced heat flux was found in late December prior to the MW in January 2019. Consistent patterns of higher heat flux forcings during the period of mWs are also shown in Fig. 5. Strahan et al. [60] also observed reduced (enhanced) wave forcing as analysed from the eddy heat flux at 100 hPa in the cold (warm) winters during the period 2005–2015.

The third and fourth panels of Fig. 5 are important as they expose the component of wave forcing responsible for the warming. The amplitudes of wavenumber 1 and 2 are analysed since they correspond to the mid-latitude planetary Rossby waves. The amplitude of planetary waves reduces as the zonal wavenumber increases. The

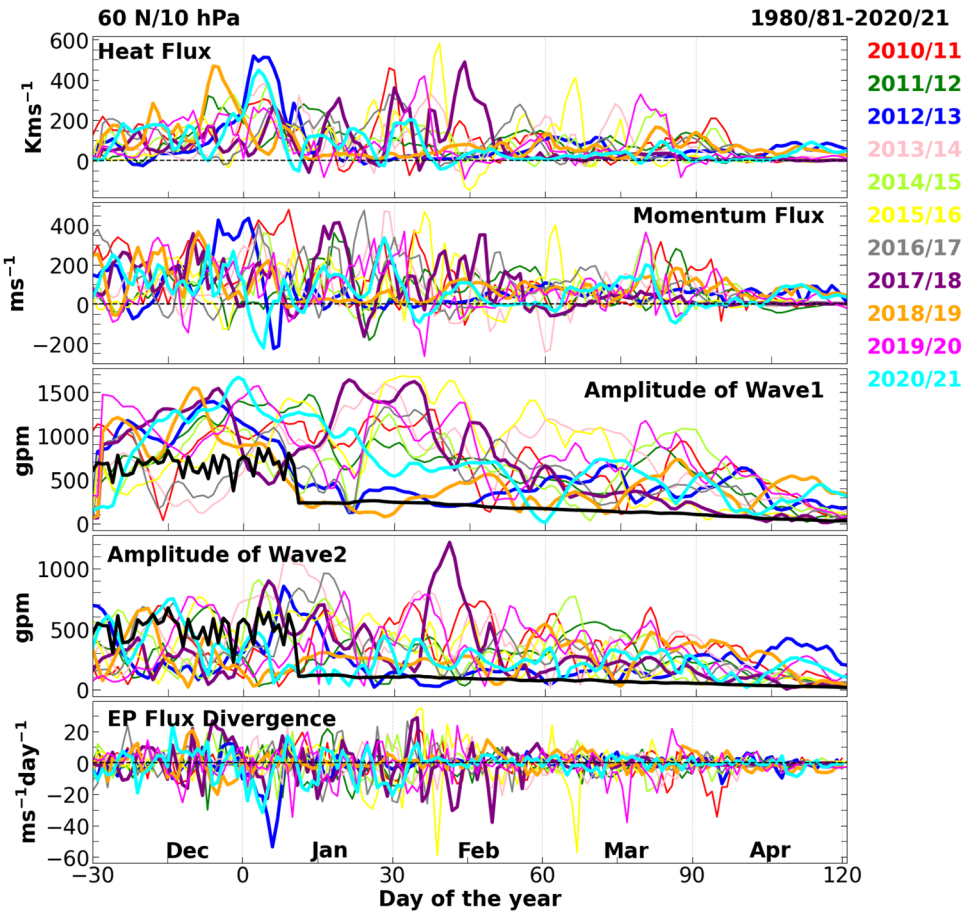

Fig. 5 Temporal evolution of meteorological parameters for the Arctic winters 2010/11–2019/20. The values are shown corresponding to 60° N latitude and 10 hPa. The dashed horizontal line indicates zero magnitude and the vertical lines indicate the separation by months. The climatology for the amplitudes of wave 1 and wave 2 is shown in the black line in the third and fourth panel

2012/13 winter was forced by high amplitudes of wave 1 (1200–1300 gpm) in December 2012, which was followed by a moderate wave 2 forcing (700–800 gpm) in early January. Therefore, the weakening of vortex began due to the influence of wave 1 and the vortex split was initiated by wave 2 [37, 61, 62].

The situation in 2017/18 winter was also similar, as wave 1 reached its highest amplitude (1500 gpm) prior to the warming and was followed by an increase in the magnitude of wave 2 (1300–1400 gpm) [44]. However, in 2018/19 and 2020/21, the forcing of wave 1 was more prominent (1500–1600 gpm). The wave 1 amplitude during the warming in 2020/21 is the highest in the past 40 years [56]. The mW in the winters 2010/11, 2011/12, 2013/14, 2015/16, 2016/17 and 2019/20 is forced by the higher amplitudes of wave 1, wave 1, waves 1 and 2, waves 1 and 2, and wave 1, respectively. High negative EP flux divergence (– 40 ms^{-1} day^{-1}) is observed in the 2012/13 winter as shown in the bottom panel of Fig. 5. Magnitudes similar to this range are also observed in the mW winter of 2015/16. A comparison of the wave amplitudes of MW and mW winters shows that the peak of wave 1 amplitude in the mW and MW years is comparable i.e., the peaks of wave 1 amplitudes in 2015/16 and 2019/20 are almost similar to that of 2017/18 and 2018/19. However, the peaks of wave 2 amplitude in the mW years are much smaller than that in the MW years. This strong wave 1 forcing from early to late February could have possibly triggered the MFW in 2015/16. Although the winter/spring is discussed in detail by several other studies, not much has been recorded about what caused this rapid amplification of planetary waves**.** Negative peaks of EP flux divergence consistent with the periods of MW is also found in the winter 2017/18 (– [20 to 30] ms^{-1} day^{-1}). However, the divergence is smaller than – 20 ms^{-1} day^{-1} for the other MW winters.

Among the external factors that influence the variability of polar vortex as discussed before in the first part of this study are the effects of ocean–atmosphere coupled processes (e.g. ENSO) and other tropospheric phenomena (e.g. QBO). A detailed description of the external forcing on the SSW winters is presented in the study of Baldwin et al. [63]. It has been observed from previous studies that the MW in 2012/13, 2017/18 and 2018/19 was favoured by the easterly phase of QBO (weak polar vortex), although the phase was not easterly in 2020/21. The winters 2012/13, 2017/18, 2018/19 and 2020/21 were preceded by a neutral ENSO, La Nina, El Nino and La Nina phases, respectively, as reported in the studies of Dai and Tan [64], Statnaia et al. [65], Lu et al. [42] and others. The weak polar vortex in the easterly phase of QBO, and the El Nino and La Nina conditions supported the occurrence of MWs in these years.

4 Major warmings and ozone

Apart from the impact of MWs on the meridional temperature gradient, zonal winds and surface conditions, the effect on polar stratosphere composition is also quite significant and has been studied in much of the previous literature [7, 63, 66, 67]. The warming causes a displacement of vortex and is also capable of changing the formation and amount of PSCs (Polar Stratospheric Clouds) responsible for ozone depletion. Henceforth, the MWs indirectly affect the amount of ozone loss in warm winters. Figure 6 compares the amount of polar cap ozone for a period of 12 years (2010–2021). The total column ozone (TCO) is obtained from satellite data and is averaged north of 63° N for January and February. The panels below in Fig. 6 show the interannual variability of the area of PSC (A_{psc}), zonal mean temperature (60°–90° N), zonal mean wind (60°–90° N), and the geopotential height (60°–90° N).

The parameters are analysed for January and December–March periods. It is observed that the highest correlation between the variables such as the zonal mean temperature, wind and the geopotential height is observed

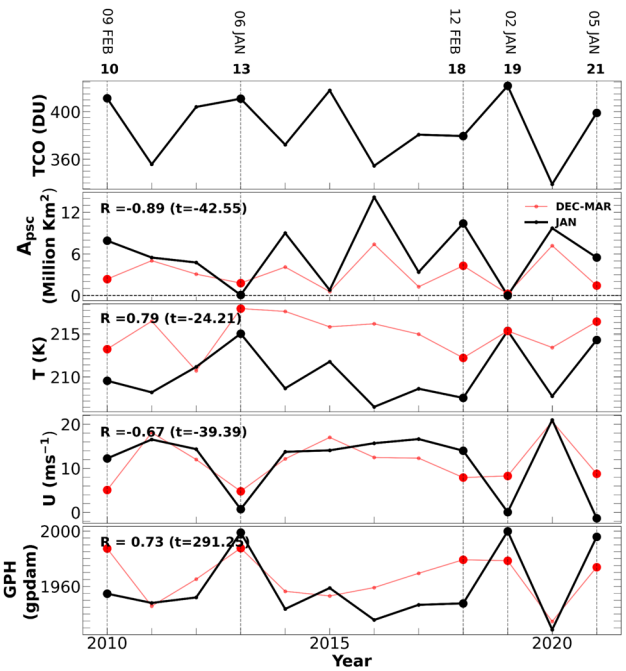

Fig. 6 The temporal evolution of total column ozone (TCO) averaged for the months January and February, Polar Stratospheric Cloud (PSC) area (A_{psc}), zonally averaged temperature (T, 60°–90° N) and winds (U, 60°–90° N) and the geopotential height (GPH, 60°–90° N). Here, the PSC area is for 460 K, and all the other variables are for 50 hPa. The top panel shows TCO. The horizontal dashed line shows the zero value of the variables and the vertical lines correspond to years with SSWs, the central date of occurrence of the warming is indicated in the top panel

Table 1 Major warming (MW) characteristics in recent Arctic winters

Arctic winter	Central date	Onset of warming	Duration of easterlies (days)	Type of warming	Prominent wave
2012/13	06 January 2013	20–24 December	22	Split	Wave 1 and 2
2017/18	12 February 2018	05–10 February	19	Split	Wave 1 and 2
2018/19	02 January 2019	15–20 December	21	Split	Wave 1
2020/21	05 January 2021	20–24 December	13	Displacement	Wave 1

The central date (the day that the westerlies at 60° N/10 hPa shifted to easterlies), whether the MW is a vortex displacement or split event, and notable wave forcing are all listed (data: MERRA 2)

in January. However, the correlation between the A_{psc} and TCO is highest for the period December–March. These values are shown in Fig. 6 together with the t-values from the analysis to show their statistical significance. The central dates for the MW winters are shown in the top panel. The TCO trend for the past four decades is estimated from the original datasets for the January–February and January–March periods. It has been found from the previous literature that 11 MWs were present in 10 winters from 2000 to 2009, among which 2001/02 was marked by the presence of two MWs (in a single winter). The TCO concentration is higher in those years with the presence of MWs (2010, 2013, 2018, 2019 and 2021). The corresponding zonal mean temperatures are also higher during these years. The TCO amount is highly correlated positively with the mean temperature in January and is statistically significant. Therefore, TCO is directly proportional to the mean temperature in January. However, this correlation reduces substantially and is slightly negative (− 0.03) when the mean temperatures between December and March are considered.

Similarly, it is observed that TCO shows a high positive correlation (0.73) with the geopotential height and its value during the MW years is higher than that of the cold winters. The zonal mean wind and the area of PSCs show inverse relationship with TCO, with the correlation of − 0.67 and − 0.89, respectively. The calculated P-value and t-value also confirm the statistical significance of these estimates. Similarly, the relatively lower temperature and higher zonal wind speed promoted unprecedented ozone depletion or lower TCO in 2010/11 and 2019/20 [51, 68]. Pommereau et al. [69] reveal that the highest percent of ozone loss during the period 1991–2017 was in the 2010/11 winter, although the winter 2019/20 was not included in their study. The corresponding A_{psc} was also the highest for the 2010/11 and 2019/20 winters. The TCO amount for the SSW years is higher than that of other years.

The highest TCO in the MW winters is observed in 2018/19, which is a direct influence of the extremely small PSC area and high temperatures. The speed of zonal winds is low and the geopotential height is moderate in that winter. In 2012/13 and 2018/19, the PSC area is marginally reduced due to the strong warming during the period and thus, the TCO amount is highest among the 12 years. The zonal wind speed is lowest in January 2021; implying a weak polar vortex due to the warming. Although 2017/18 had a MW, the TCO is lower than that of other MW winters because of the relatively stronger polar vortex and higher A_{psc} (in January) during the period. Since, most MWs occurred in January and February; the amount of ozone is also found to be increased consistently during the period. Therefore, the timing of maximum TCO varies directly with the occurrence of a MW. The ozone trend analysed for the past four decades (1979–2020) reveals that the TCO is decreasing at − 0.08 DU/year for the period January–March, but increasing at 0.30 DU/year in January–February, although these values are not statistically significant. It is probable that the increasing trend during the January–February period is influenced by the presence of frequent SSWs.

5 Conclusions

We have characterised the SSWs for the past 11 winters (2010/11–2020/21) in the Arctic. The occurrence of major warming was identified in 4 winters; namely 2012/13, 2017/18, 2018/19 and 2020/21. These events have a subsequent influence on the surface weather and there are ample shreds of evidence that imply the same [57, 61, 70]. The cold air outbreak following the major warming of 2017/18 was titled as the 'Beast from the East' due to the extreme cold winters that resulted after the warming in the Arctic [71]. Therefore, it is important to conduct a comprehensive study of these events together with the mW events to improve the predictability of these events in the coming years. We found that, among the MW winters, the most severe warming was manifested in 2012/13. This severity is identified by the steep temperature rise (30 K) and the longest persistence of easterly winds in that winter. The easterlies extended to altitudes as low as 75 hPa.

The PV maps revealed that 2012/13, 2017/18 and 2018/19 were split events, but a vortex displacement in 2020/21. The amplitude of wave forcings showed a combined forcing of waves 1 and 2 in 2012/13 and 2017/18. The amplitude of wave 1 increases significantly before the central date of warming and the amplitude of wave 2 increases during the event. The vortex split in 2018/19 was forced by a higher amplitude of wave 1 than wave 2. This was quite contrary to the usual associations of wave 2 forcings with the split type vortex. Previous studies have shown that the frequency of SSWs has been on the rise in the Northern Hemisphere and was observed to be about 1.1 MWs/winter in 1998/99–2009/10. According to our analysis, the frequency has reduced to 0.36 MWs/winter from 2010/11 to 2020/21, and 0.74 MWs/winter from 1998/99 to 2020/21, although the range of the frequency can depend on the type of dataset used.

The examination of the relationship between total column ozone and the occurrence of SSWs since 2000 revealed that the amount of ozone is directly proportional to the presence of warmings. A high negative correlation is noticed between TCO and the area of the PSCs. The highest TCO was observed in the MW of 2018/19 (420 DU) in agreement with the smallest PSC area (< 2 million km^2) in that winter. Despite the development of mWs in other winters, 2010/11, 2015/16 and 2019/20 were unusually cold for much of the early winter and henceforth, was responsible for significantly higher PSC area (6–8 million km^2) and smaller TCO (340–350 DU). Nevertheless, the ozone loss further was restricted by the mW events that occurred in the latter part of those winters. Therefore, our study also helps to analyse the connection between ozone and the SSWs.

Acknowledgements We thank the Indian Institute of Technology Kharagpur, for facilitating the study. RR thanks Head (R. Sajeev) Department of Physical Oceanography, Cochin University of Science and Technology, Kochi, India for his help and support during her study there. JK acknowledges his gratitude to Chairman CORAL and Director IIT Kgp for their continued support and help.

Author contribution RR: Formal analysis, Investigation, Visualization, Writing—original draft, Writing—review and editing. JK: Conceptualization, Methodology, Formal analysis, Investigation, Visualization, Writing—original draft, Writing—review and editing, Project administration.

Funding This study received no funding.

Data availability The data utilised in this study is open to the public. On request, the analysed data can be shared. The MERRA-2 data are on: https://gmao.gsfc.nasa.gov/reanalysis/MERRA-2/, the CAMS data are on: https://atmosphere.copernicus.eu/data. The total ozone column data obtained from the TOMS, OMI and OMPS satellite dataset from the NASA ozone watch site: https://ozonewatch.gsfc.nasa.gov/. The NCEP data are available on https://psl.noaa.gov/data/gridded/data.ncep.reanalysis.html.

Declarations

Conflicts of interest The authors declare no conflict of interest associated with this study.

References

1. Scherhag R (1952) Die explosions artige Stratosph ¨arenerwarmug des Spa¨twinters 1951/52. Ber Deut Wetterdieustes 6:51–63
2. WMO/IQSY (1964) International Years of the Quiet Sun (IQSY), 1964–1965: alert messages with special references to stratwarms. Secretariat of the WMO WMO/IQSY Report 6, 19 pp. +3 appendices
3. Labitzke K (1977) Interannual variability of the winter stratosphere in the Northern Hemisphere. Mon Weather Rev 105:762–770. https://doi.org/10.1175/1520-46.0493(1977)105%3c0762:ivotws%3e2.0.co;2
4. Andrews DG, Holton JR, Leovy CB (1987) Middle atmosphere dynamics. Academic Press Inc., Cambridge
5. WMO (1978) Abridged final report of the seventh session (27 February–10 March 1978; Manila, Philippines) of the Commission for Atmospheric Sciences, WMO report 509, 113 pp, ISBN 978-92-631-0509-7
6. McInturff RM (1978) Stratospheric warmings: synoptic, dynamic and general-circulation aspects, Technical Report NASA-RP-1017, NASA Reference Publ., Washington, DC
7. Kuttippurath J, Nikulin G (2012) A comparative study of the major sudden stratospheric warmings in the Arctic winters 2003/2004–2009/2010. Atmos Chem Phys 12(17):8115–8129. https://doi.org/10.5194/acp-12-8115-2012
8. Butler AH, Seidel DJ, Hardiman SC, Butchart N, Birner T, Match A (2015) Defining sudden stratospheric warmings. Bull Am Meteorol Soc 96(11):1913–1928. https://doi.org/10.1175/BAMS-D-13-00173.1
9. Butler AH, Gerber EP (2018) Optimizing the definition of a sudden stratospheric warming. J Clim 31(6):2337–2344
10. Kuttippurath J, Godin-Beekmann S, Lefèvre F, Goutail F (2010) Spatial, temporal, and vertical variability of polar stratospheric ozone loss in the Arctic winters 2004/2005–2009/2010. Atmos Chem Phys 10:9915–9930. https://doi.org/10.5194/acp-10-9915-2010
11. Limpasuvan V, Thompson DWJ, Hartmann DL (2004) The life cycle of the Northern Hemisphere sudden stratospheric warmings. J Clim 17:2584–2596. https://doi.org/10.1175/1520-0442(2004)017¡2584:TLCOTN¿2.0.CO;2

12. Charlton AJ, Polvani LM (2007) A new look at stratospheric sudden warmings. Part i: climatology and modeling benchmarks. J Clim 20:449–469. https://doi.org/10.1175/JCLI3996.1
13. Schoeberl MR (1978) Stratospheric warmings: observations and theory. Rev Geophys 16(4):521–538. https://doi.org/10.1029/rg016i004p00521
14. Cohen J, Jones J (2011) Tropospheric precursors and stratospheric warmings. J Clim 24:6562–6572. https://doi.org/10.1175/2011JCLI4160.1
15. Zhang Y, Yi Y, Ren X et al (2021) (2021) Statistical characteristics and long-term variations of major sudden stratospheric warming events. J Meteorol Res 35:416–427. https://doi.org/10.1007/s13351-021-0166-3
16. Bancalá S, Krüger K, Giorgetta M (2012) The preconditioning of major sudden stratospheric warmings. J Geophys Res. https://doi.org/10.1029/2011JD016769
17. Choi H, Kim B, Choi W (2019) Type classification of sudden stratospheric warming based on pre- and postwarming periods. J Clim 32(8):2349–2367
18. Loon HV, Jenne RL, Labitzke KB (1973) Zonal harmonic standing waves. J Geophys Res 78:4463–4471
19. Holton JR, Tan HC (1980) The influence of the equatorial quasi-biennial oscillation on the global circulation at 50 mb. J Atmos Sci 37(10):2200–2208
20. Hu D, Guan Z, Tian W, Ren R (2018) Recent strengthening of the stratospheric Arctic vortex response to warming in the central North Pacific. Nat Commun 9:1697. https://doi.org/10.1038/s41467-018-04138-3
21. Domeisen DI, Garfinkel CI, Butler AH (2019) The teleconnection of El Niño Southern Oscillation to the stratosphere. Rev Geophys 57:5–47. https://doi.org/10.1029/2018RG000596
22. Hu D, Guan Z, Guo Y, Lu C, Jin D (2019) Dynamical connection between the stratospheric Arctic vortex and sea surface temperatures in the North Atlantic. Clim Dyn 53:6979–6993. https://doi.org/10.1007/s00382-019-04971-2
23. Zhang et al (2020) North American cold events following sudden stratospheric warming in the presence of low Barents-Kara Sea sea ice. Environ Res Lett. https://doi.org/10.1088/1748-9326/abc215
24. Dimdore-Miles O, Gray L, Osprey S (2021) Origins of multi-decadal variability in sudden stratospheric warmings. Weather Clim Dyn 2:205–231. https://doi.org/10.5194/wcd-2-205-2021
25. Mitchell DM, Osprey SM, Gray LJ, Butchart N, Hardiman SC, Charlton-Perez AJ, Watson P (2012) The effect of climate change on the variability of the Northern Hemisphere stratospheric polar vortex. J Atmos Sci 69:2608–2618. https://doi.org/10.1175/JAS-D-12-021.1
26. Ayarzagüena B, Charlton-Perez AJ, Butler AH, Hitchcock P, Simpson IR, Polvani LM et al (2020) Uncertainty in the response of sudden stratospheric warmings and stratosphere-troposphere coupling to quadrupled CO_2 concentrations in cmip6 models. J Geophys Res Atmos. https://doi.org/10.1029/2019JD032345
27. Cohen J, Pfeiffer K, Francis JA (2018) Warm Arctic episodes linked with increased frequency of extreme winter weather in the United States. Nat Commun 9:869. https://doi.org/10.1038/s41467-018-02992-9
28. Goncharenko LP, Harvey VL, Liu H, Pedatella NM (2021) Sudden stratospheric warming impacts on the ionosphere–thermosphere system. In: Huang C, Lu G, Zhang Y, Paxton LJ (eds) Ionosphere dynamics and applications. https://doi.org/10.1002/9781119815617.ch16
29. Butler AH, Polvani LM (2011) El Niño, La Niña, and stratospheric sudden warmings: a reevaluation in light of the observational record. Geophys Res Lett 38:L13807. https://doi.org/10.1029/2011GL048084
30. Manney GL, Krüger K, Sabutis JL, Sena SA, Pawson S (2005) The remarkable 2003–2004 winter and other recent warm winters in the Arctic stratosphere since the late 1990s. J Geophys Res 34:387–396. https://doi.org/10.1029/2004JD005367
31. Orsolini YJ, Urban J, Murtagh DP, Lossow S, Limpasuvan V (2010) Descent from the polar mesosphere and anomalously high stratopause observed in 8 years of water vapor and temperature satellite observations by the Odin Sub-Millimeter Radiometer. J Geophys Res 115:D12305. https://doi.org/10.1029/2009JD013501
32. Labitzke K, Kunze M (2009) On the remarkable Arctic winter in 2008/2009. J Geophys Res 114:D00I02. https://doi.org/10.1029/2009JD012273
33. Kuttippurath J, Kleinböhl A, Sinnhuber M, Bremer H, Küllmann H, Notholt J, Godin-Beekmann S, Tripathi O, Nikulin G (2011) Arctic ozone depletion in 2002–2003 measured by ASUR and comparison with POAM observations. J Geophys Res 116:D22305. https://doi.org/10.1029/2011JD016020
34. Coy L, Eckermann S, Hoppel K (2019) Planetary wave breaking and tropospheric forcing as seen in the stratospheric sudden warming of 2006. J Atmos Sci 66:495–507. https://doi.org/10.1175/2008JAS2784.1
35. Cao C, Chen YH, Rao J, Liu SM, Li SY, Ma MH, Wang YB (2019) Statistical characteristics of major sudden stratospheric warming events in CESM1-WACCM: a comparison with the JRA55 and NCEP/NCAR reanalyses. Atmosphere 10:519. https://doi.org/10.3390/atmos10090519
36. Liu SM, Chen YH, Rao J, Cao C, Li SY, Ma Mhu H, Wang YB (2019) Parallel comparison of major sudden stratospheric warming events in CESM1-WACCM and CESM2-WACCM. Atmosphere 10(11):679. https://doi.org/10.3390/atmos10110679
37. Coy L, Pawson S (2015) The major stratospheric sudden warming of January 2013: analyses and forecasts in the GEOS-5 data assimilation system. Mon Weather Rev 143:491–510
38. Nath D, Chen W, Zelin C et al (2016) Dynamics of 2013 Sudden Stratospheric Warming event and its impact on cold weather over Eurasia: role of planetary wave reflection. Sci Rep 6:24174. https://doi.org/10.1038/srep24174
39. Rao J, Ren RC, Chen HS, Yu YY, Zhou Y (2018) The stratospheric sudden warming event in February 2018 and its prediction by a climate system model. J Geophys Res Atmos 123:13332–13345. https://doi.org/10.1029/2018JD028908
40. Rao J, Garfinkel CI, Chen HS, White IP (2019) The 2019 New Year stratospheric sudden warming and its real-time predictions in multiple S2S models. J Geophys Res Atmos 124(21):11155–11174. https://doi.org/10.1029/2019JD030826
41. Ma Z, Gong Y, Zhang SD, Luo JH, Zhou QH, Huang CM, Huang KM (2020) Comparison of stratospheric evolution during the major sudden stratospheric warming events in 2018 and 2019. Earth Planet Phys 4(5):1–11. https://doi.org/10.26464/epp2020044
42. Lu Q, Rao J, Liang Z, Guo D, Luo J, Liu S, Wang C, Wang T (2021) The sudden stratospheric warming in January 2021. Environ Res Lett. https://doi.org/10.1088/1748-9326/ac12f4
43. Gelaro R, McCarty W, Suárez MJ, Todling R, Molod A, Takacs L et al (2017) The modern-era retrospective analysis for research and applications, version 2 (MERRA-2). J Clim 30(14):5419–5454. https://doi.org/10.1175/JCLI-D-16-0758.1
44. Black RX, McDaniel BA, Robinson WA (2006) Stratosphere–troposphere coupling during spring onset. J Clim 19:4891–4901. https://doi.org/10.1175/JCLI3907.1
45. Black RX, McDaniel BA (2007) The dynamics of Northern Hemisphere stratospheric final warming events. J Atmos Sci 64:2932–2946. https://doi.org/10.1175/JAS3981
46. Jucker M (2020) Script and data for scaling of Eliassen-Palm flux vectors. Atmos Sci Lett. https://doi.org/10.1002/asl.1020

47. Palmer TN (1981) Diagnostic study of a wavenumber-2 stratospheric sudden warming in a transformed Eulerian-mean formalism. J Atmos Sci 38:844–855. https://doi.org/10.1175/1520-0469%281981%29038%3C0844%3ADSOAW
48. McIntyre ME, Palmer TN (1983) Breaking planetary waves in the stratosphere. Nature 305:593–600. https://doi.org/10.1038/305593a0
49. Nash ER, Newman PA, Rosenfield JE, Schoeberl MR (1996) An objective determination of the polar vortex using Ertel's potential vorticity. J Geophys Res Atmos 101(D5):9471–9478. https://doi.org/10.1029/96jd00066
50. Karpechko AY, Charlton-Perez A, Balmaseda M, Tyrrell N, Vitart F (2018) Predicting sudden stratospheric warming 2018 and its climate impacts with a multimodel ensemble. Geophys Res Lett 45:13538–13546. https://doi.org/10.1029/2018GL081091
51. Manney G, Santee M, Rex M et al (2011) Unprecedented Arctic ozone loss in 2011. Nature 478:469–475. https://doi.org/10.1038/nature10556
52. Kuttippurath J, Feng W, Müller R, Kumar P, Raj S, Gopikrishnan GP, Roy R (2021) Exceptional loss in ozone in the Arctic winter/spring of 2019/2020. Atmos Chem Phys 21:14019–14037. https://doi.org/10.5194/acp-21-14019-2021
53. Manney GL, Lawrence ZD, Santee ML, Livesey NJ, Lambert A, Pitts MC (2015) Polar processing in a split vortex: Arctic ozone loss in early winter 2012/2013. Atmos Chem Phys 15:5381–5403. https://doi.org/10.5194/acp-15-5381-2015
54. Manney GL, Lawrence ZD (2016) The major stratospheric final warming in 2016: dispersal of vortex air and termination of Arctic chemical ozone loss. Atmos Chem Phys 16:15371–15396. https://doi.org/10.5194/acp-16-15371-2016
55. Lee SH, Butler AH (2019) The 2018–2019 Arctic stratospheric polar vortex. Weather. https://doi.org/10.1002/wea.3643
56. Lee SH (2021) The January 2021 sudden stratospheric warming. Weather 76:135–136. https://doi.org/10.1002/wea.3966
57. Lü Z, Li F, Orsolini YJ, Gao Y, He S (2020) Understanding of European cold extremes, sudden stratospheric warming, and siberian snow accumulation in the winter of 2017/18. J Clim 33(2):527–545
58. Li Y, Tian W, Xie F et al (2018) The connection between the second leading mode of the winter North Pacific sea surface temperature anomalies and stratospheric sudden warming events. Clim Dyn 51:581–595. https://doi.org/10.1007/s00382-017-3942-0
59. Attard HE, Rios-Berrios R, Guastini CT, Lang AL (2016) Tropospheric and stratospheric precursors to the January 2013 sudden stratospheric warming. Mon Weather Rev 144(4):1321–1339
60. Strahan SE, Douglass AR, Steenrod SD (2016) Chemical and dynamical impacts of stratospheric sudden warmings on Arctic ozone variability. J Geophys Res Atmos 121:11,836-11,851. https://doi.org/10.1002/2016JD025128
61. Liu Y, Zhang Y (2014) Overview of the major 2012–2013 Northern Hemisphere stratospheric sudden warming: evolution and its association with surface weather. J Meteorol Res 28:561–575. https://doi.org/10.1007/s13351-014-3065-z
62. Tripathi OP, Baldwin M, Charlton-Perez A, Charron M et al (2016) Examining the predictability of the stratospheric sudden warming of January 2013 using multiple NWP systems. Mon Weather Rev 144(5):1935–1960
63. Baldwin MP, Ayarzagüena B, Birner T, Butchart N, Butler AH, Charlton-Perez AJ et al (2021) Sudden stratospheric warmings. Rev Geophys 59:e2020RG000708. https://doi.org/10.1029/2020RG000708
64. Dai Y, Tan B (2016) The western Pacific pattern precursor of major stratospheric sudden warmings and the ENSO modulation. Environ Res Lett. https://doi.org/10.1088/1748-9326/aa538
65. Statnaia IA, Karpechko AY, Järvinen HJ (2020) Mechanisms and predictability of sudden stratospheric warming in winter 2018. Weather Clim Dyn 1:657–674. https://doi.org/10.5194/wcd-1-657-2020
66. Sagi K, Pérot K, Murtagh D, Orsolini Y (2017) Two mechanisms of stratospheric ozone loss in the Northern Hemisphere, studied using data assimilation of Odin/SMR atmospheric observations. Atmos Chem Phys 17:1791–1803. https://doi.org/10.5194/acp-17-1791-2017
67. de la Cámara A, Abalos M, Hitchcock P, Calvo N, Garcia RR (2018) Response of Arctic ozone to sudden stratospheric warmings. Atmos Chem Phys 18:16499–16513. https://doi.org/10.5194/acp-18-16499-2018
68. Manney GL, Livesey NJ, Santee ML, Froidevaux L, Lambert A, Lawrence ZD et al (2020) Record-low Arctic stratospheric ozone in 2020: MLS observations of chemical processes and comparisons with previous extreme winters. Geophys Res Lett. https://doi.org/10.1029/2020GL089063
69. Pommereau JP, Goutail F, Pazmino A, Lefèvre F, Chipperfield MP et al (2018) Recent Arctic ozone depletion: is there an impact of climate change? C R Geosci. https://doi.org/10.1016/j.crte.2018.07.009
70. Xie J, Hu J, Xu H, Liu S, He H (2020) Dynamic diagnosis of stratospheric sudden warming event in the boreal winter of 2018 and its possible impact on weather over North America. Atmosphere 11:438. https://doi.org/10.3390/atmos11050438
71. King AD, Butler AH, Jucker M, Earl NO (2019) Rudeva I (2019) Observed relationships between sudden stratospheric warmings and European climate extremes. J Geophys Res Atmos 124:13943–13961. https://doi.org/10.1029/2019JD030480